New insight into the fission process

from experiments

with relativistic heavy ions

Aleksandra Kelic
Maria Valentina Ricciardi
Karl-Heinz Schmidt

GSI Darmstadt

Lay out

- Introduction
- Characteristics of the inverse-kinematics approach
- Multimodal fission after electromagnetic excitations
- Nuclide production in spallation fission reactions
- Model developments
- Future

Previous experimental knowledge on low-energy fission

Fission channels

- variation with E^*
- variation with A and Z of the fissioning system (rather limited choice)

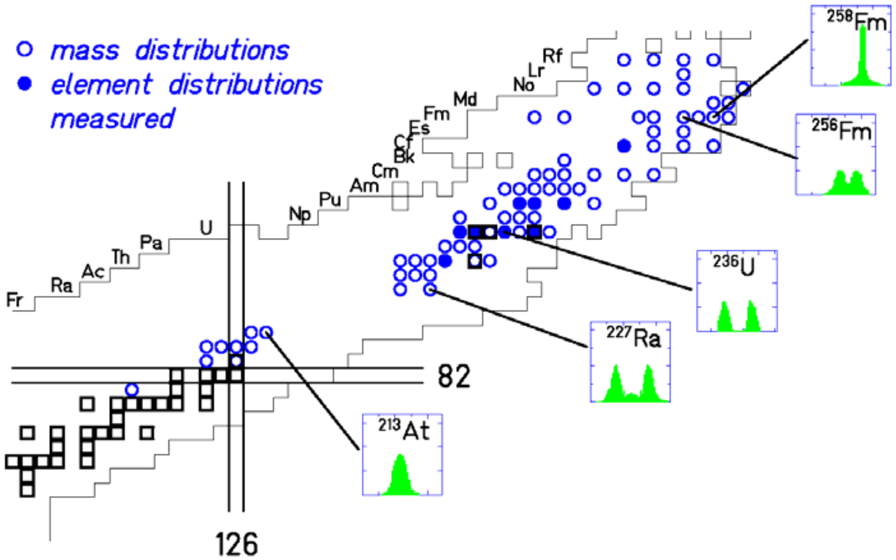

Even-odd effect in the Z yields

- variation with E^*
- variation with $Z^2/A^{1/3}$

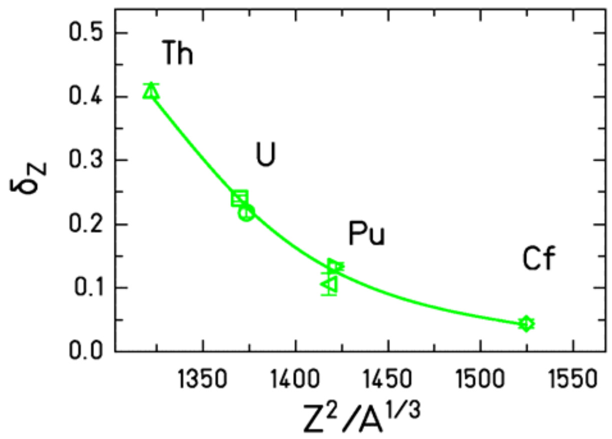

Neutron yields,
Kinetic energy,
…

Our method; the inverse-kinematics approach

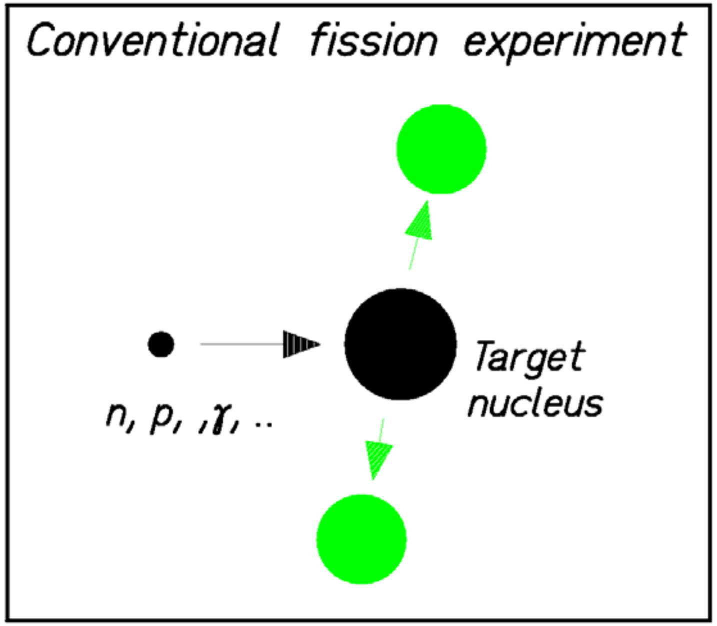

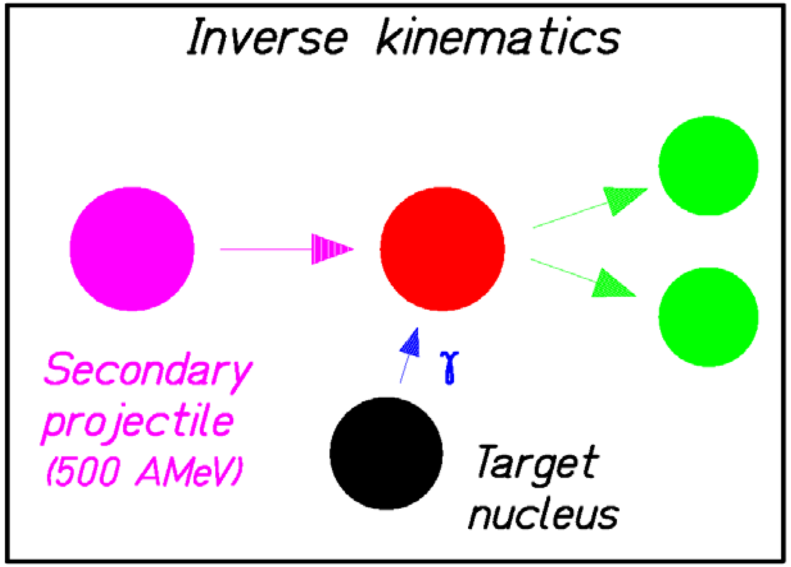

Fission of target nuclei

Fission of projectile nuclei

1. **Better means for detection by the high velocity of the products!**
2. **Short-lived nuclei accessible!**

Experimental progress

brought by the inverse-kinematics approach

Methods for the detection of fission fragments

- discovery of fission (1939) ► *chemical identification in Z*
- kinetic energy of the fragments ► *ionisation chamber*
- cumulative yields (after ß decay) ► *gamma spectroscopy*
- ≈ A_1 and A_2 ► *double E, double ToF*
- elements *Z* ► *X rays*
- *A* and *Z* of the light fragments ► *Spectrographe (Lohengrin) + energy loss* (limited to target material with long half-lives and thermal neutrons)
- ***A* and *Z* ► in-flight identification *in inverse kinematics***
- **Z_1 and Z_2 ► in-flight identification *in inverse kinematics***
- ***A* and *Z* ► high-resolution mass measurement (*traps*), normalisation?**

Choice of the fissionning system

- Primordial nuclides (^{238}U, ^{235}U, ^{232}Th) ► *target*
- Fission reactors (neutron capture - ß) ► *target* (long-lived nuclides)
- Nuclear explosions (neutrons capture – ß) ► *target* (long-lived nuclides)
- Products of direct reactions ► *target* (long-lived nuclides)
- **Projectile fragmentation (A < 238) ► *beam* (half-life > 100 ns)**

Excitation mechanisms:

- neutrons (thermal, fast, mono energetic)
- electrons
- photons (bremsstrahlung, mono energetic)
- protons and other charged particles (fusion, direct reactions)
- spontaneous fission
- **electromagnetic and nuclear interaction *in inverse kinematics***
    - nuclear target (GSI) -> distribution in E^* (≈ RGD in e.m. and $E^* \uparrow$ in nucl.)
    - electron collider – ions (FAIR) -> well-defined E^*

The installations of GSI actually used

for fission studies

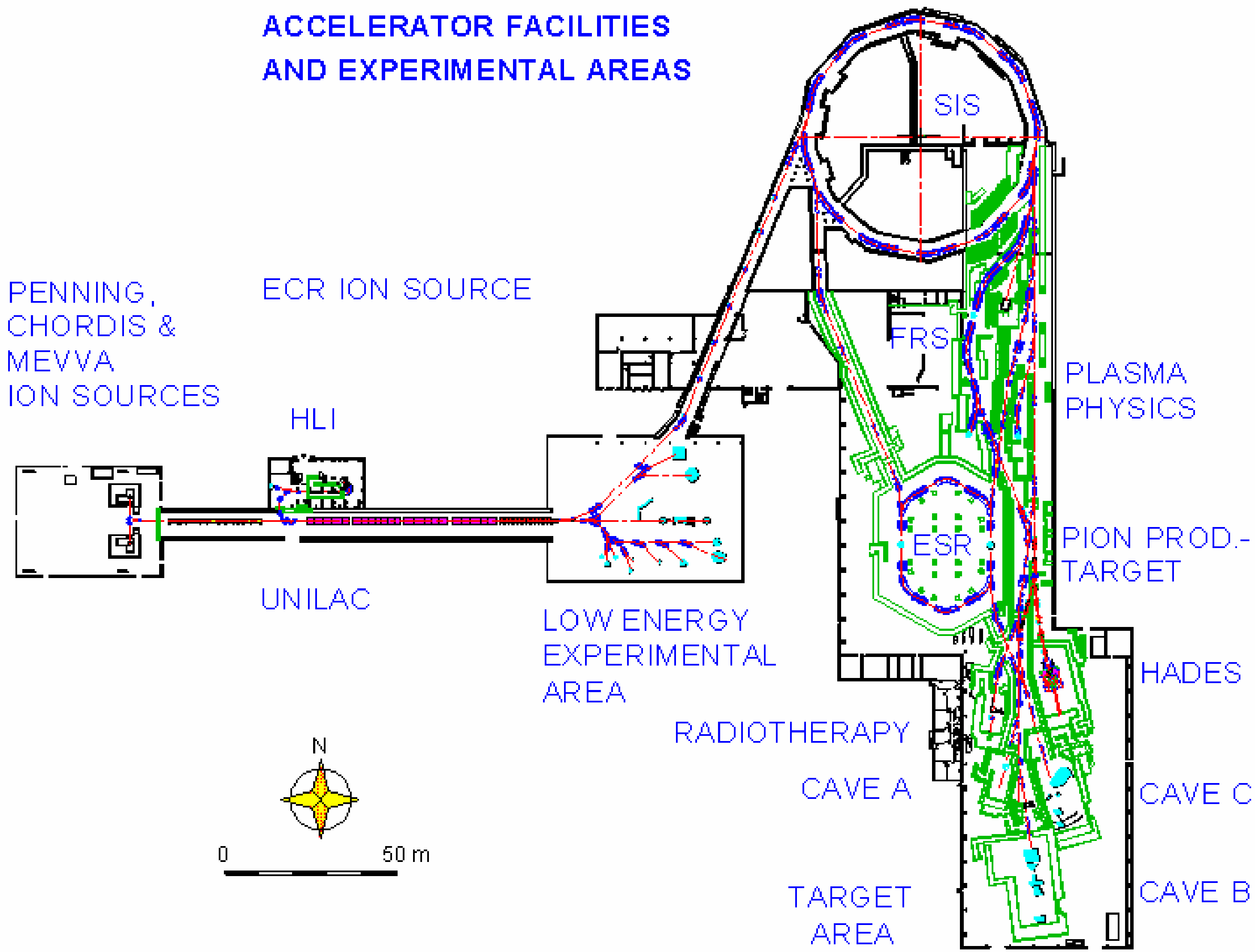
ACCELERATOR FACILITIES
AND EXPERIMENTAL AREAS
SIS
PENNING,
CHORDIS &
MEVVA
ION SOURCES
ECR ION SOURCE
HLI
FRS
PLASMA
PHYSICS
ESR
PION PROD.-
TARGET
UNILAC
LOW ENERGY
EXPERIMENTAL
AREA
HADES
RADIOTHERAPY
CAVE A
CAVE C
N
0
50 m
TARGET
AREA
CAVE B

1. Z identification of both fission fragments

(Applicable also to short-lived radioactive fissile systems)

Double ionisation chamber – time-of-flight wall

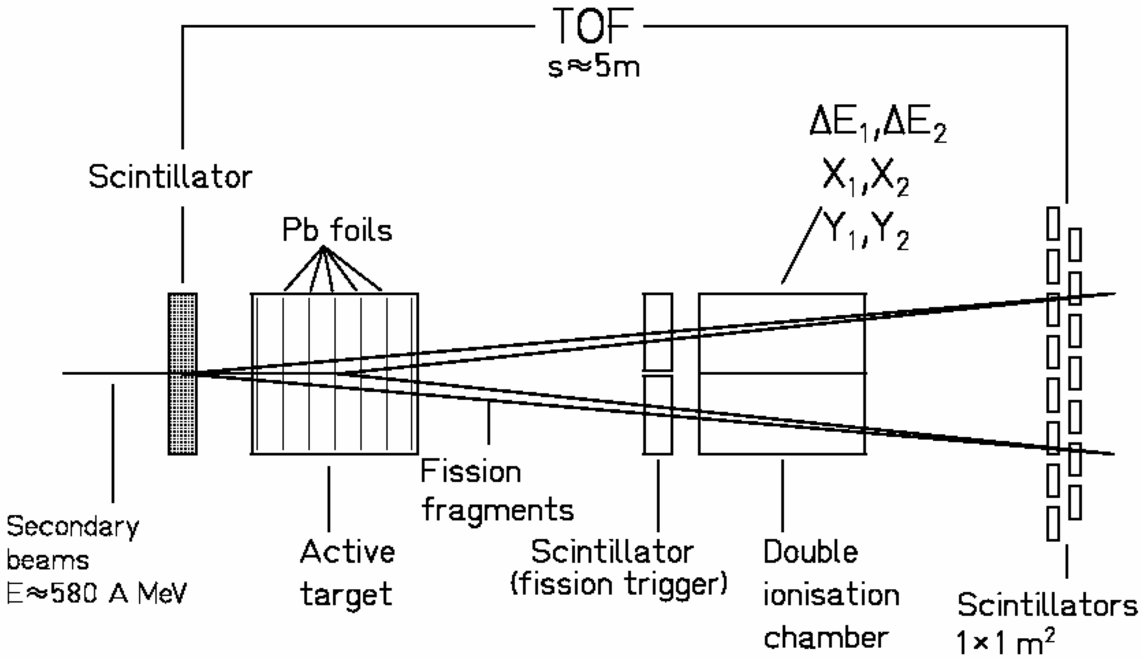

The detectors

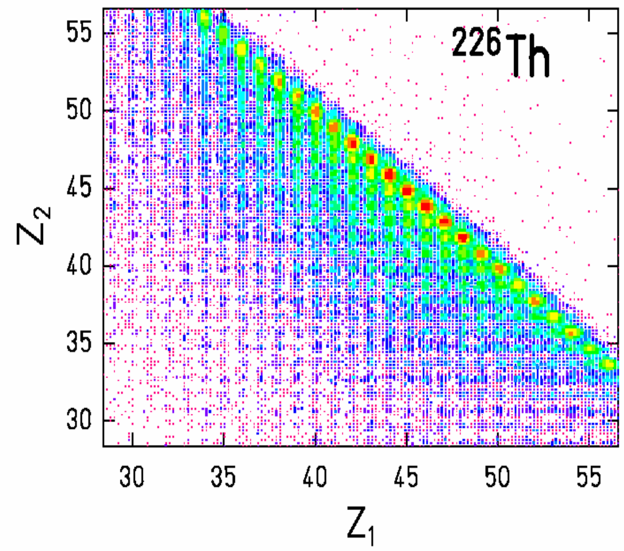

Identification of both fragments in Z

Z distributions

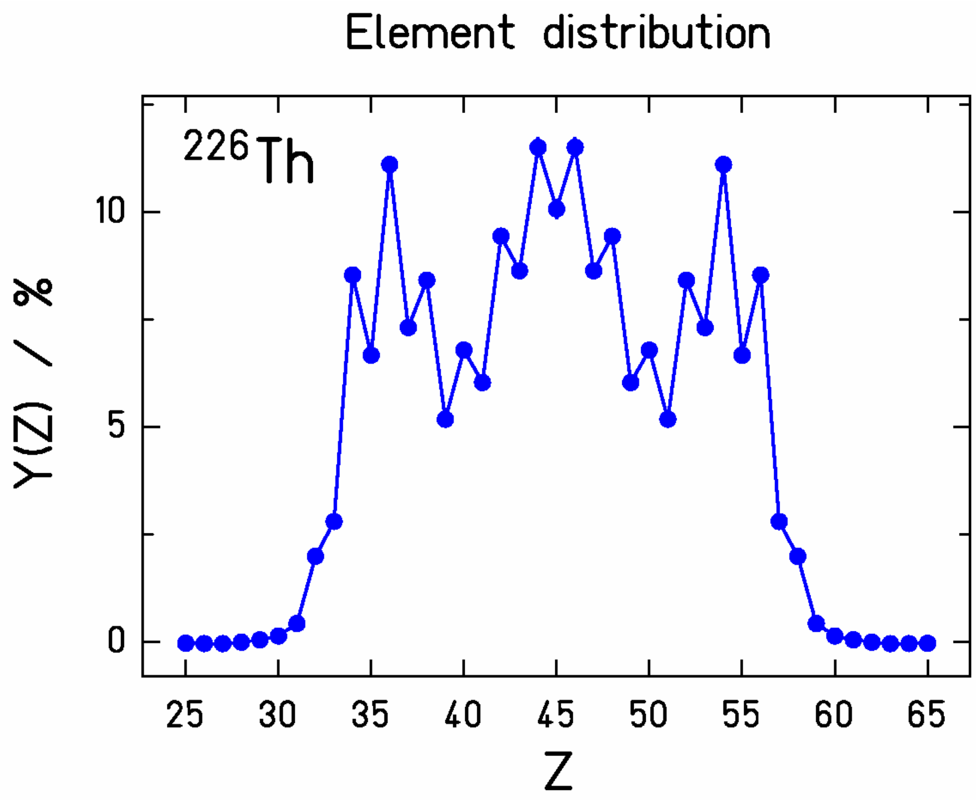

Fission after excitation of the giant dipole resonance (E* ≈ 11 MeV)

($t_{1/2}$ of ^{226}Th = 31 minutes !)

Appearance of an even-odd effect for odd-Z fissioning nuclei

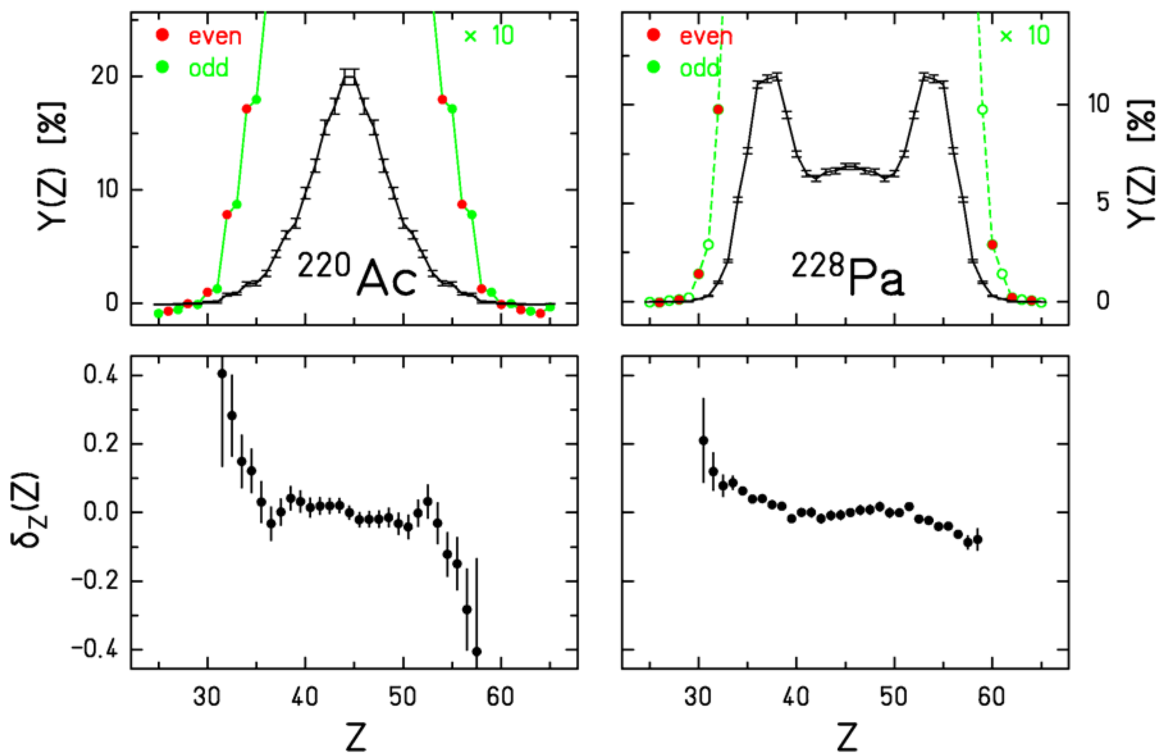

Statistical explication by the phase space available for one individual proton in the two fragments at scission ($g \sim A$).

Bimodal fission of the neutron-deficient actinides

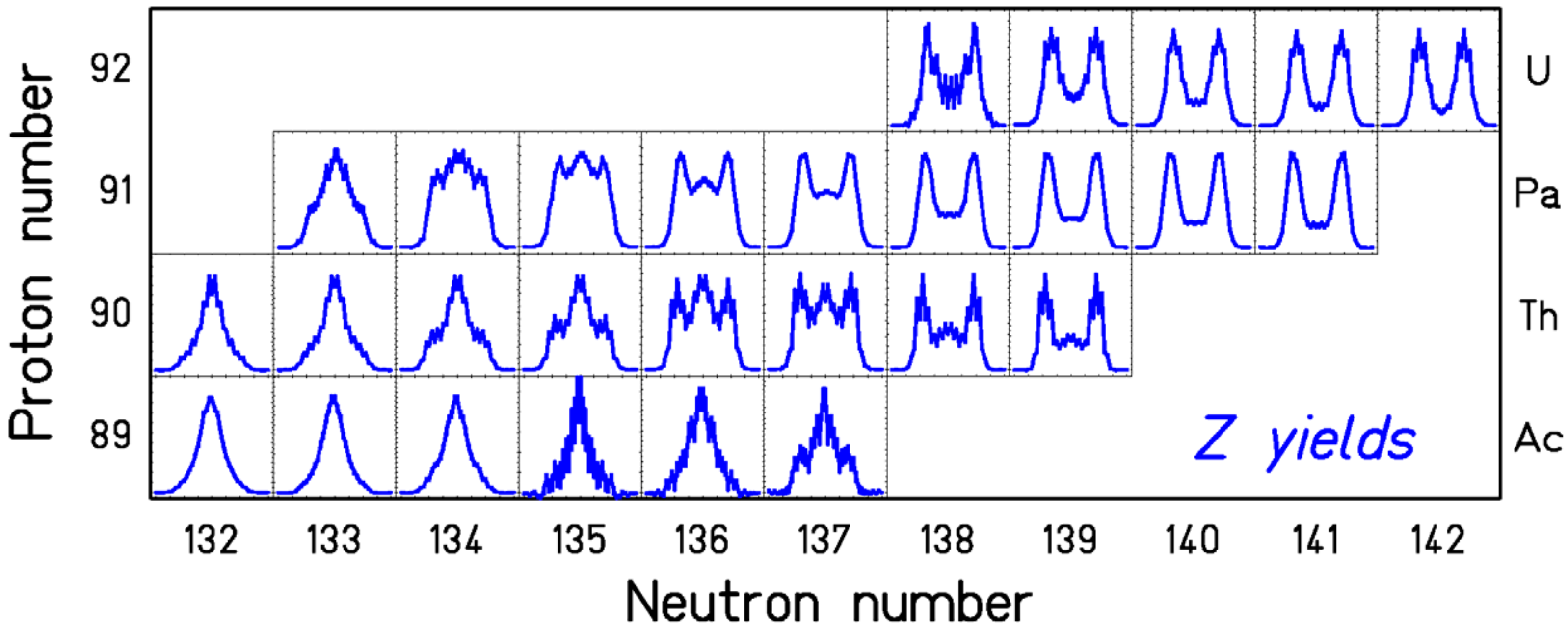

***Z* distributions after excitation of the GDR (*E** ≈ 11 MeV)**
(K.-H. Schmidt et al., NPA 665 (2000) 221)

General view on the experimental results on fission of light actinides by use of secondary beams of radioactive nuclides.

Improved experimental knowledge

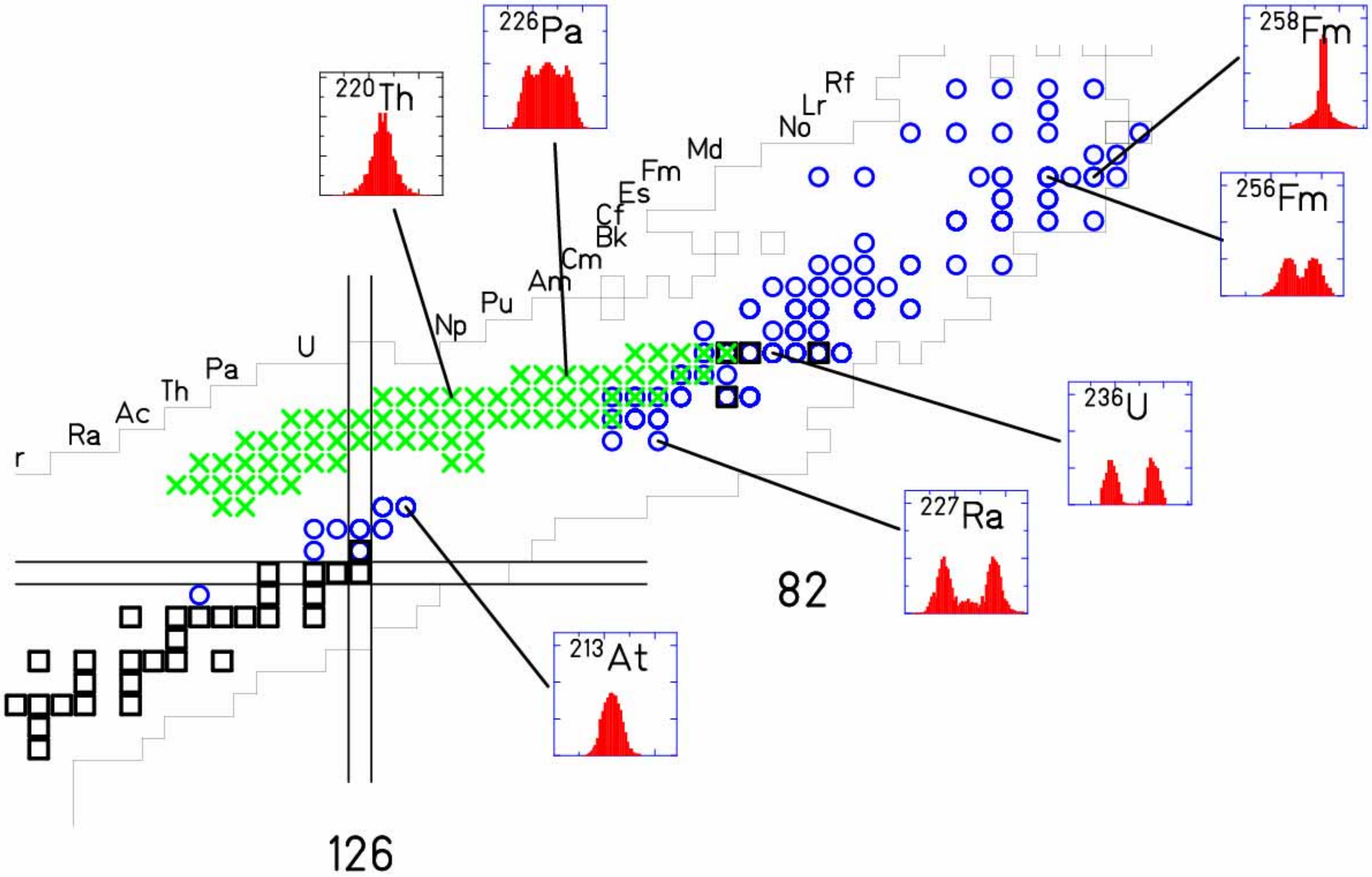

2. Full identification of <u>one</u> fission fragments in *Z* <u>and</u> *A*

The fragment separator as a magnetic spectrometer

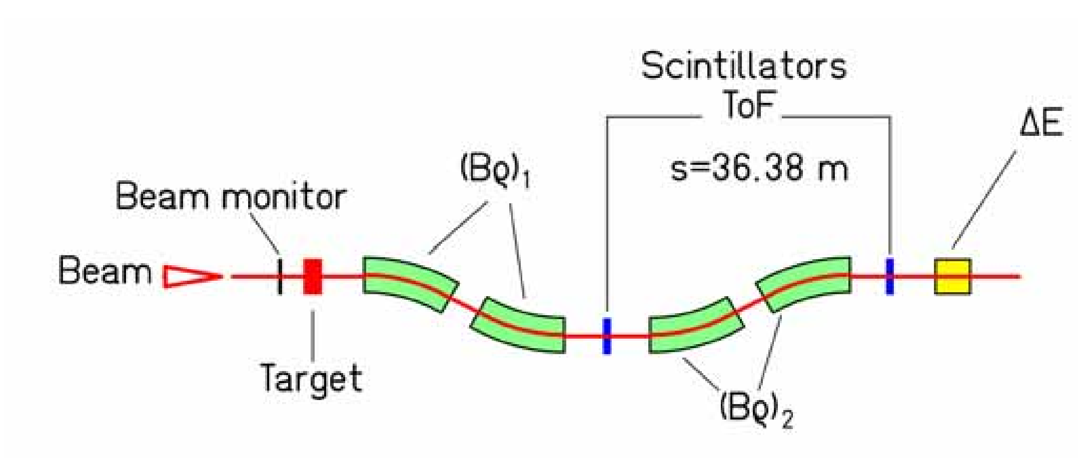

Spectrometer

^{238}U (1*A* GeV) + ^{1}H

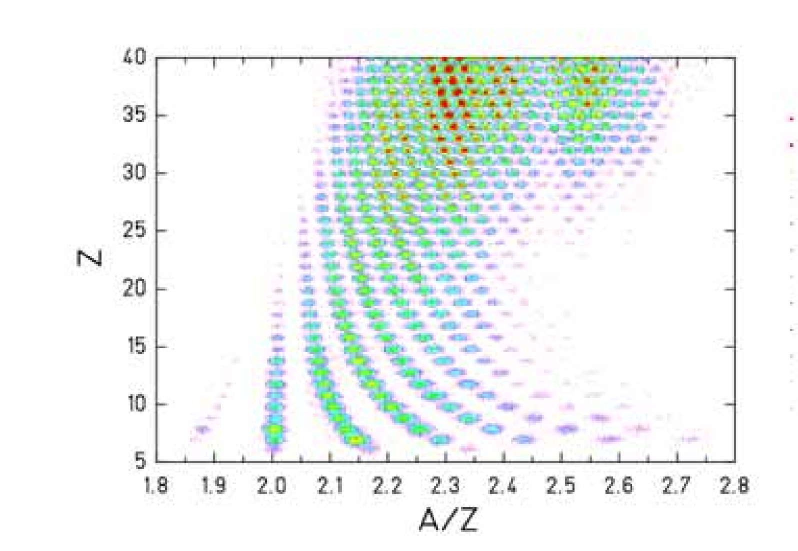

Nuclide identification
(M. V. Ricciardi)

Resolution $p/\Delta p \approx 2000$.
Acceptance $\Delta B\rho / B\rho = 3\%$ and Θ_{max}=15 mr.
Identification in Z and A by magnetic deflection, tracking, *ToF* and ΔE.
Basic equations: $B\rho = m_0 \mathbf{A}\, c\, \beta\, \gamma\, /\, (e\, \mathbf{Z})$ and $\Delta E \propto \mathbf{Z}^2 / v^2$

Kinematical signature of fission

(^{238}U + ^{1}H in Ti container)

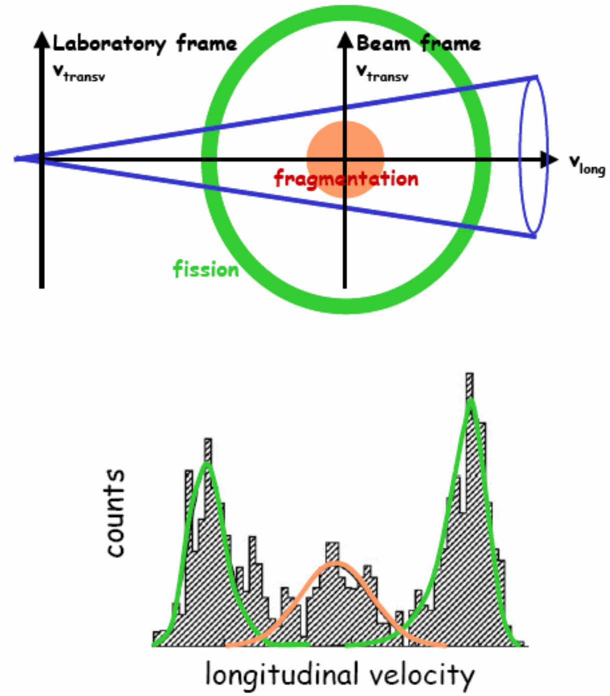

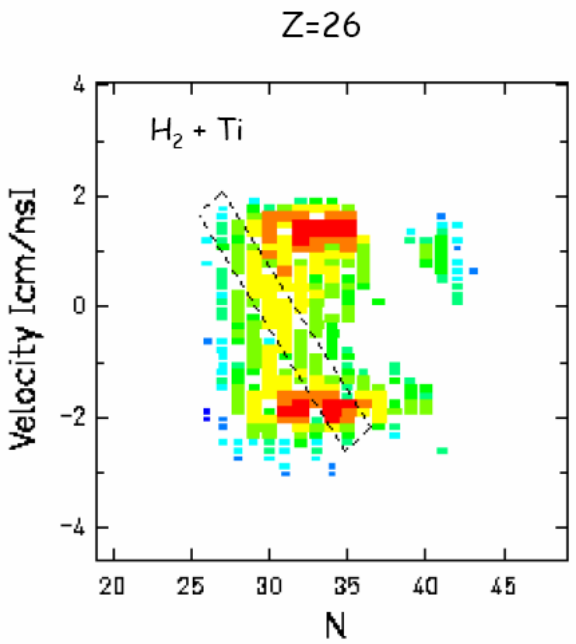

The Coulomb repulsion of the fission fragments causes a double-humped profile in the measured velocity distribution.

Experimental progress by inverse-kinematics method

Example: Fission of lead induced by ≈ 500 MeV protons

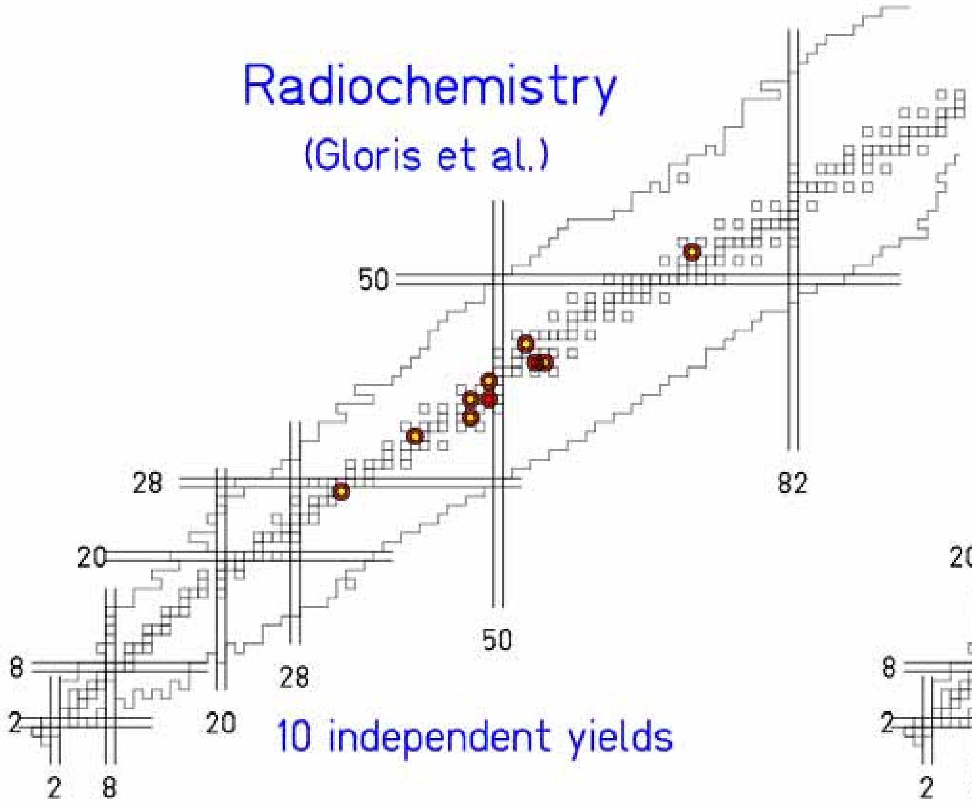

protons (553 MeV) on lead

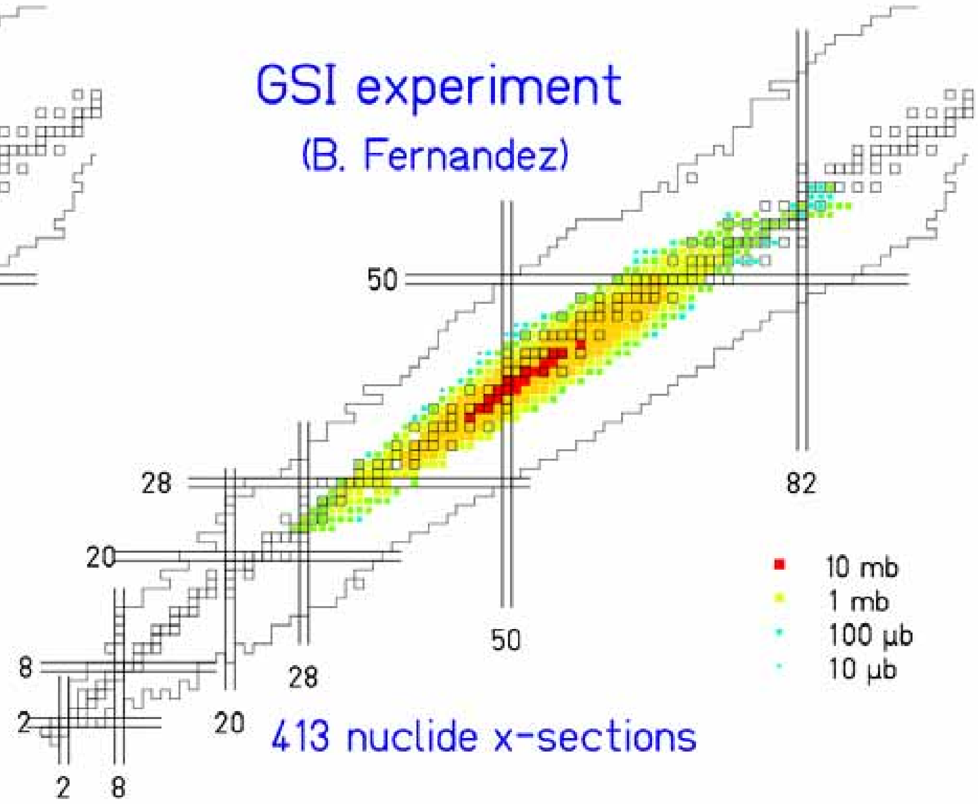

^{208}Pb (500 A MeV) on hydrogen

Some systems investigated (7732 data points)

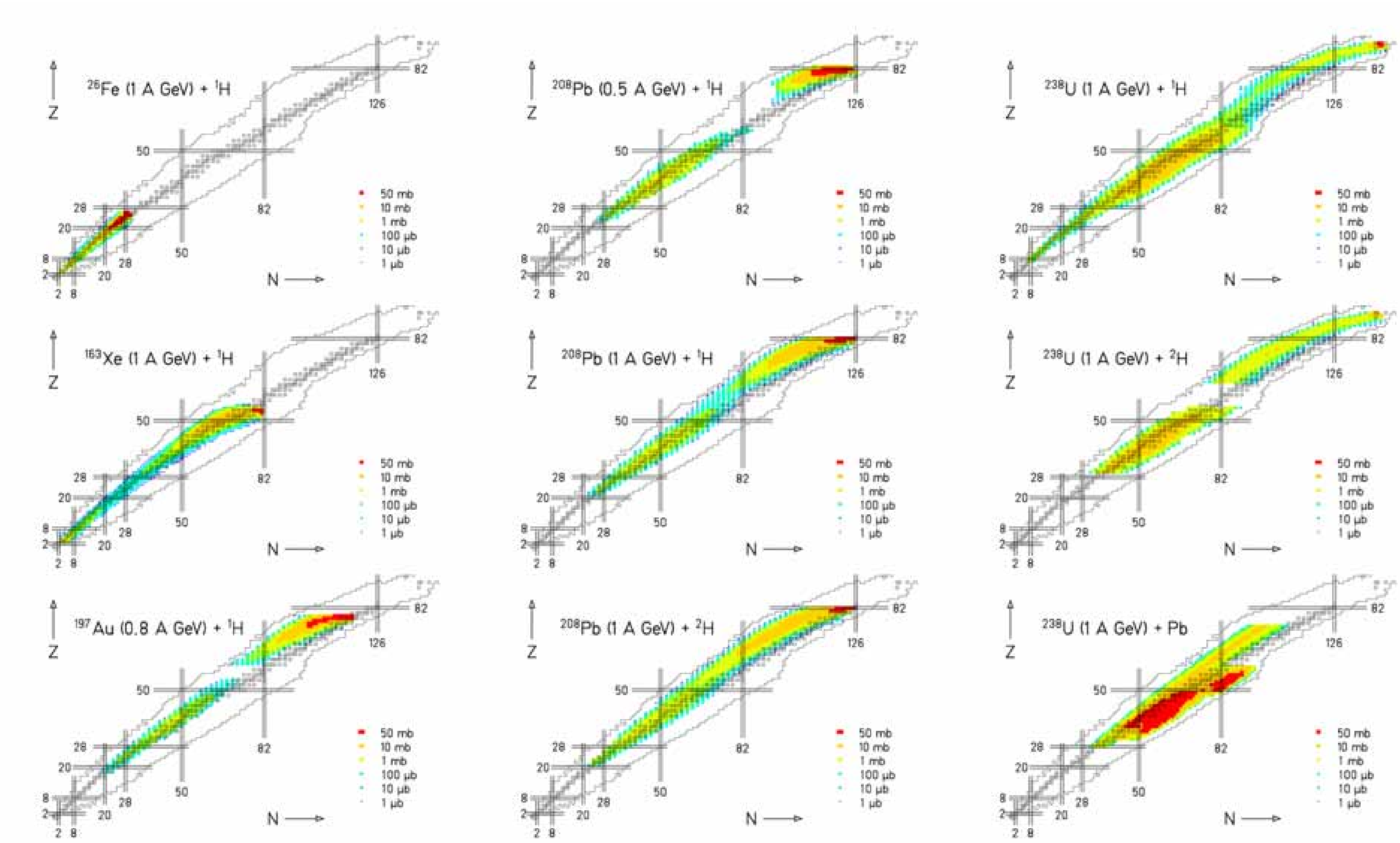

List of systems investigated

^{56}Fe (0.3 to 1.5 *A* GeV) + ^{1}H	C. Villagrasa, PhD thesis P. Napolitani et al., PRC 70 (2004) 054607
^{136}Xe(0.2 to 1 *A* GeV) + ^{1,2}H	P. Napolitani, PhD thesis L. Giot, in preparation M. Fernandez, in preparation
^{197}Au (0.8 *A* GeV) + ^{1}H	F. Rejmund et al., NPA 683 (2001) 540 J. Benlliure et al., NPA 683 (2001) 513
^{208}Pb (1 *A* GeV) + ^{1,2}H	T. Enqvist et al., NPA 686 (2001) 481 T. Enqvist et al., NPA 703 (2002) 435 A. Kelić et al., PRC 70 (2004) 064608
^{208}Pb (0.5 *A* GeV) + ^{1}H	B. Fernandez et al., NPA 747 (2005) 227 L. Audouin et al., arXiv-nucl-ex/0503021
^{238}U (1 *A* GeV) + ^{1,2}H	M. V. Ricciardi et al., arXiv-nucl-ex/0508027 M. Bernas et al., NPA 725 (2003) 213 M. Bernas et al., submitted J. Taieb et al., NPA 724 (2003) 413 J. Pereira, PhD thesis E. Casarejos, PhD thesis P. Armbruster et al., PRL 93 (2004) 212701
^{238}U (1 *A* GeV) + Pb	T. Enqvist et al., NPA 658 (1999) 47

Applications

- Spallation neutron source
- ADS (accelerator-driven system) for nuclear waste

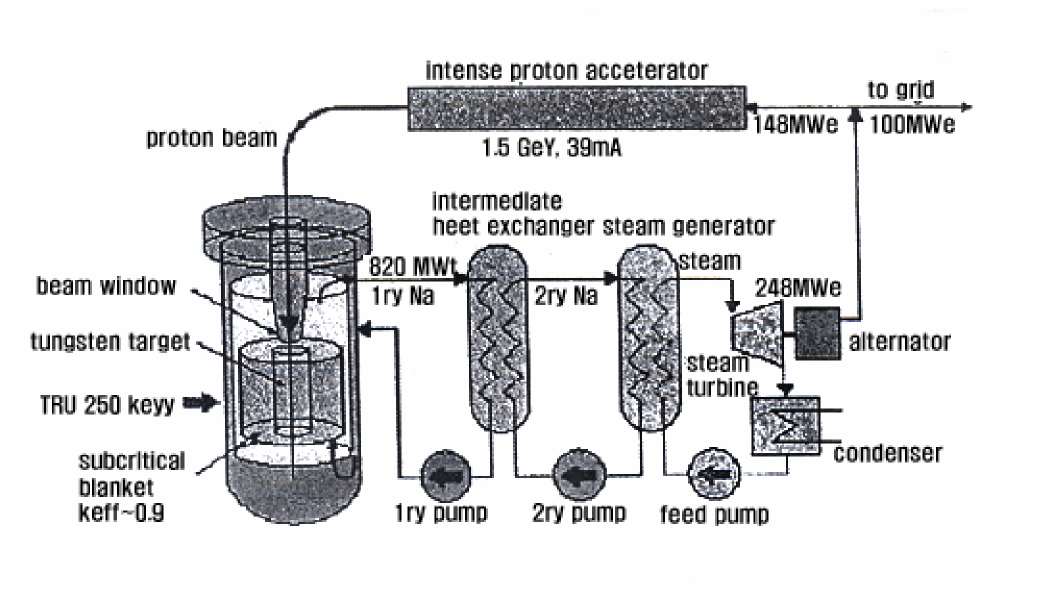

-

- Production of secondary beams (EURISOL)

Comparison of two systems

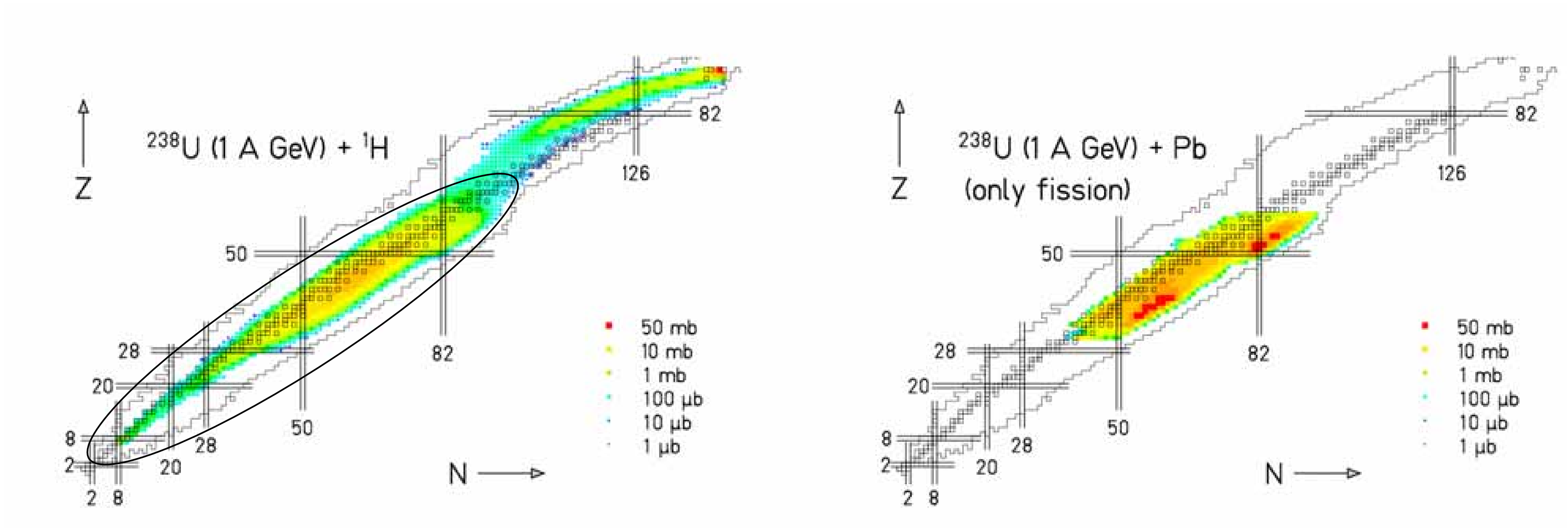

Fission of ^{238}U induced in a hydrogen and a lead target:

Very different nuclide distributions.

Can we understand this?

Model developments (ABRABLA code)

- Collision stage
- Abrasion model

- Evaporation stage
- Weisskopf approach with extension to IMFs

- Fission
- Semiempirical macroscopic-microscopic approach

  (Time-dependent fission-decay width,
  statistical population of fission channels,
  evaporation from CN, saddle-scission, fragments)

Systematics of mass width for high-energy fission (Rusanov et al.)

702 RUSANOV *et al.*

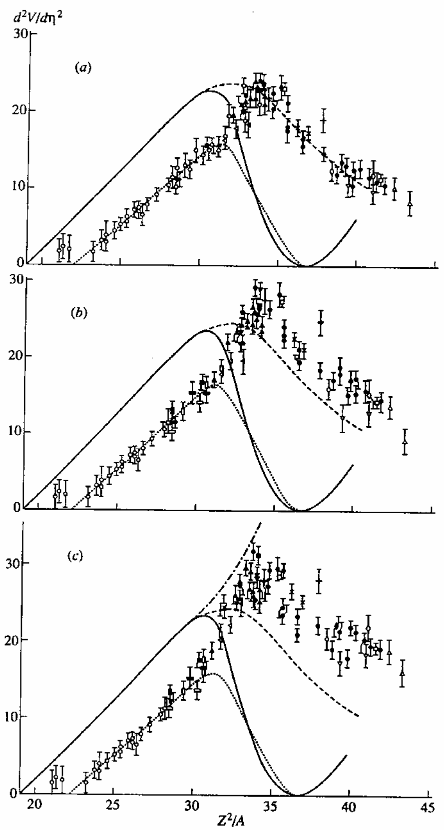

Fig. 8. Experimental dependences of the stiffness $d^2V/d\eta^2$ on Z^2/A at $l = 0$ for various definitions of θ_i^j: (*a*) θ_{sp}^{eff1}, (*b*) θ_{sp}^{eff2}, and (*c*) θ_{sc}^{eff3}. Open circles represent experimental data from [2], and open squares show the results of our analysis for $^{205,206}At$ and $^{260}104$ nuclei. The notation for the remaining points is given in Table 3. Solid, dotted, and dashed curves illustrate the results of theoretical calculations performed, respectively, in [14] for the saddle point with LDM parameters from [62], in [2] for the saddle point according the LDM formulated in [12], and in [14] according to the diffusion model with parameters from [62]. The dash-dotted curve in Fig. 8*c* represents the results of the calculation from [14] for the scission point with parameters from [62].

PHYSICS OF ATOMIC NUCLEI Vol. 60 No. 5 1997

$$\sigma_A{}^2 = \frac{T}{c_A}$$

Population of mass-asymmetry degree of freedom follows relations of statistical model.

c_A is the curvature of the potential at the elongation where the decision on the A distribution is made.

To be extended to low energies!

Structural effects on potential important at low energies

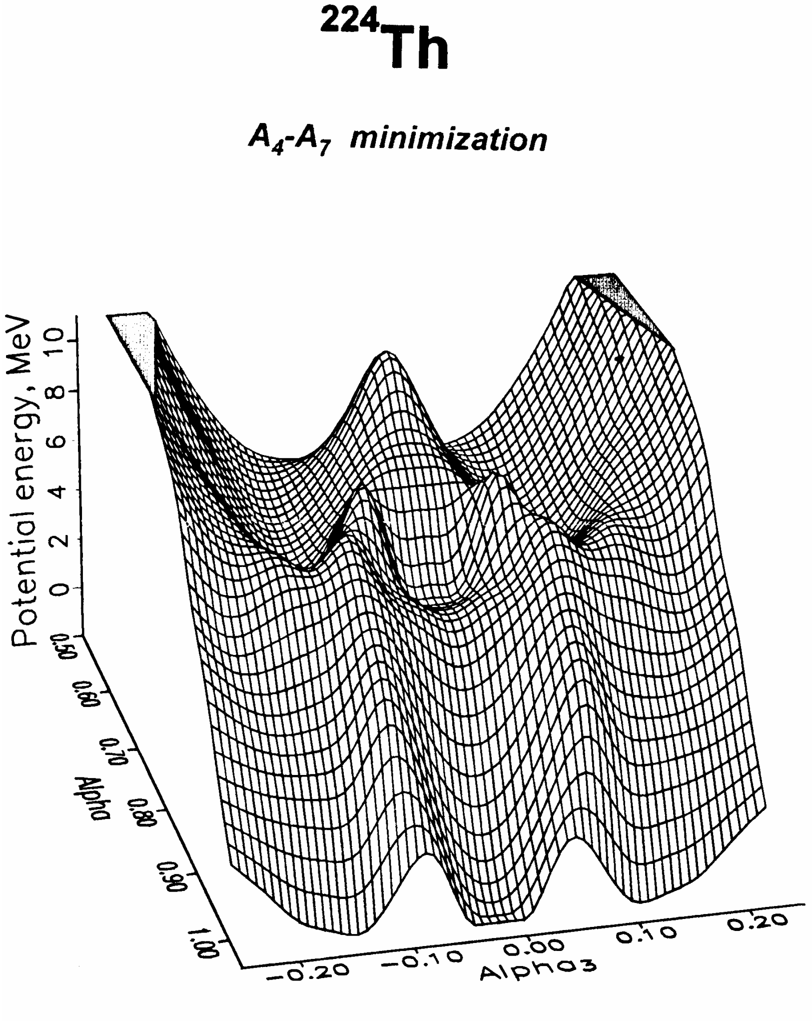

Shell effects responsible for fission channels.

Parabolic potential (Rusanov): macroscopic potential

Shell corrections can be deduced from measured mass distributions

(as Rusanov et al. did for deducing the macroscopic potential)

← Calculation by Pashkevich

Shell effects of fragments

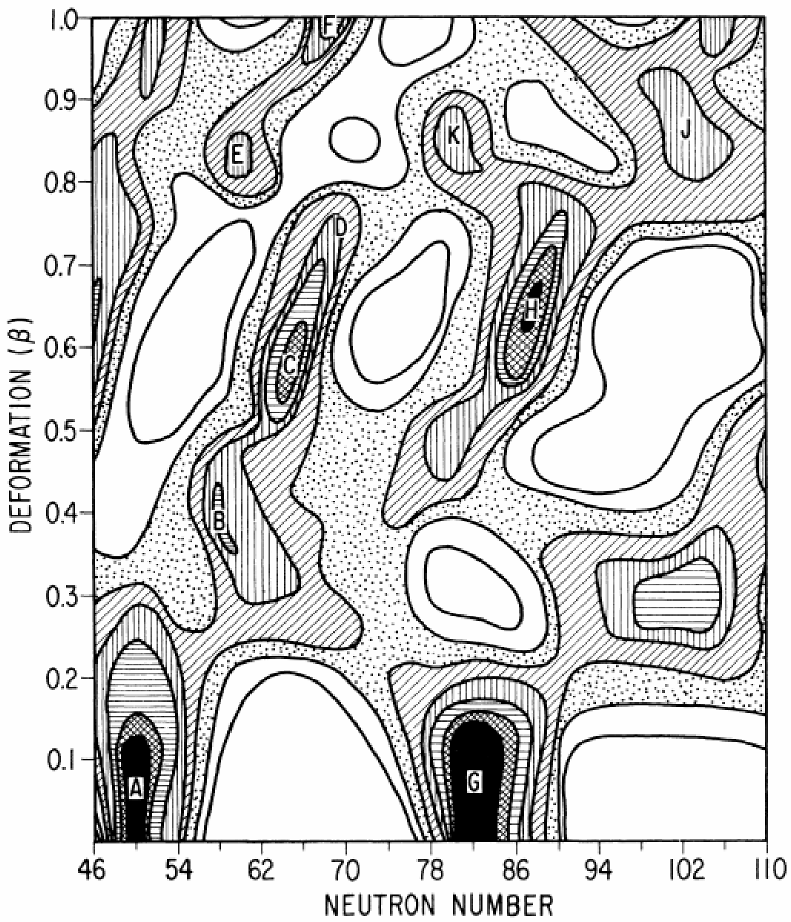

FIG. 1. Neutron-shell corrections calculated as a function of deformation (β) and neutron number. The contours are plotted at 1 MeV intervals with the black regions (representing the strongest shell corrections) containing all values lower than -4 MeV and the inner white region (representing the weakest shell corrections) containing all values greater than +2 MeV. The contours do not include any pairing or liquid-drop terms. The letters refer to particular shell regions as described in the text.

Shells on the potential-energy from outer saddle to scission are rather properties of the fragments!

(Maruhn & Greiner, Pashkevich)

← Shell-model calculations. Wilkins et al.

Variation of potential due to shells

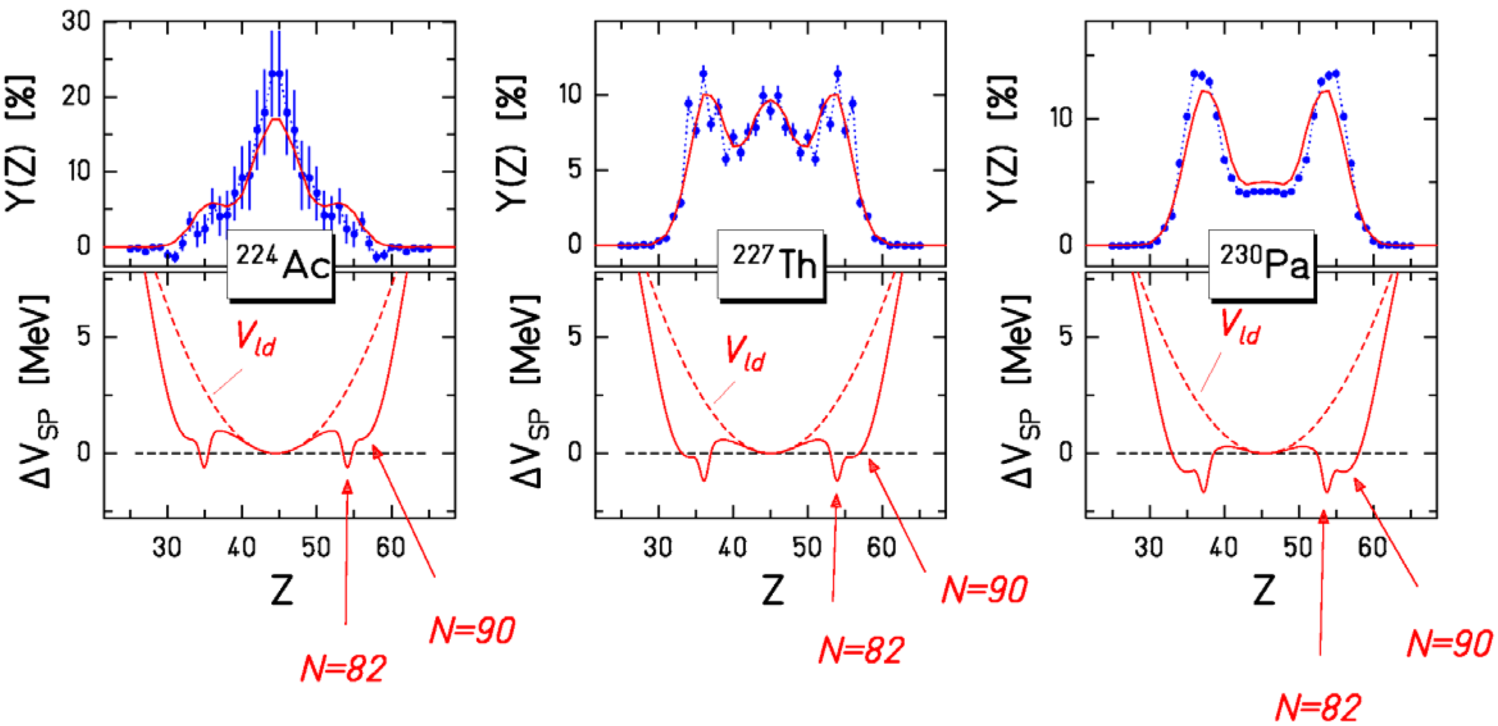

Transition from single-humped to double-humped distributions investigated experimentally (K.-H. Schmidt et al., NPA 665 (2000) 221) **and explained by macroscopic (CN) and microscopic (nascent fragments) properties of the potential-energy landscape near saddle**

Essential ingredient: Vanishing of shell effects with increasing excitation energy.

(J. Benlliure et al., Nucl. Phys. A 628 (1998) 458).

Evolution of the fission *Z* distribution as a function of *A* and *E**

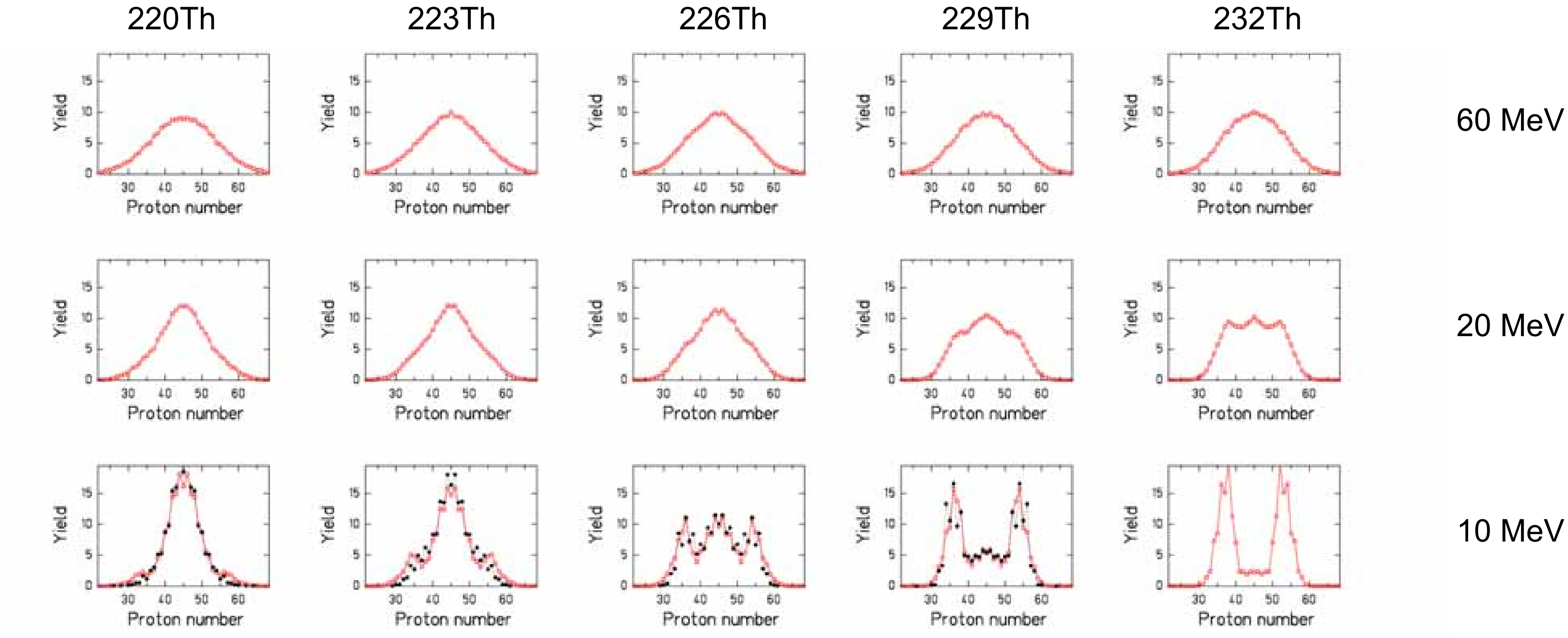

red: PROFI calculations, **black:** experimental data (K.-H. Schmidt et al., NPA 665 (2000) 221)

Nuclide distribution in spallation: superposition of fission from different nuclei at different *E.**

Variation with A: checked by comparison with experiment.

Variation with E*: predicted by systematics of microscopic calculations.

Reproduction ^{238}U + n (1.7 .. 13 MeV) (same parameters!)

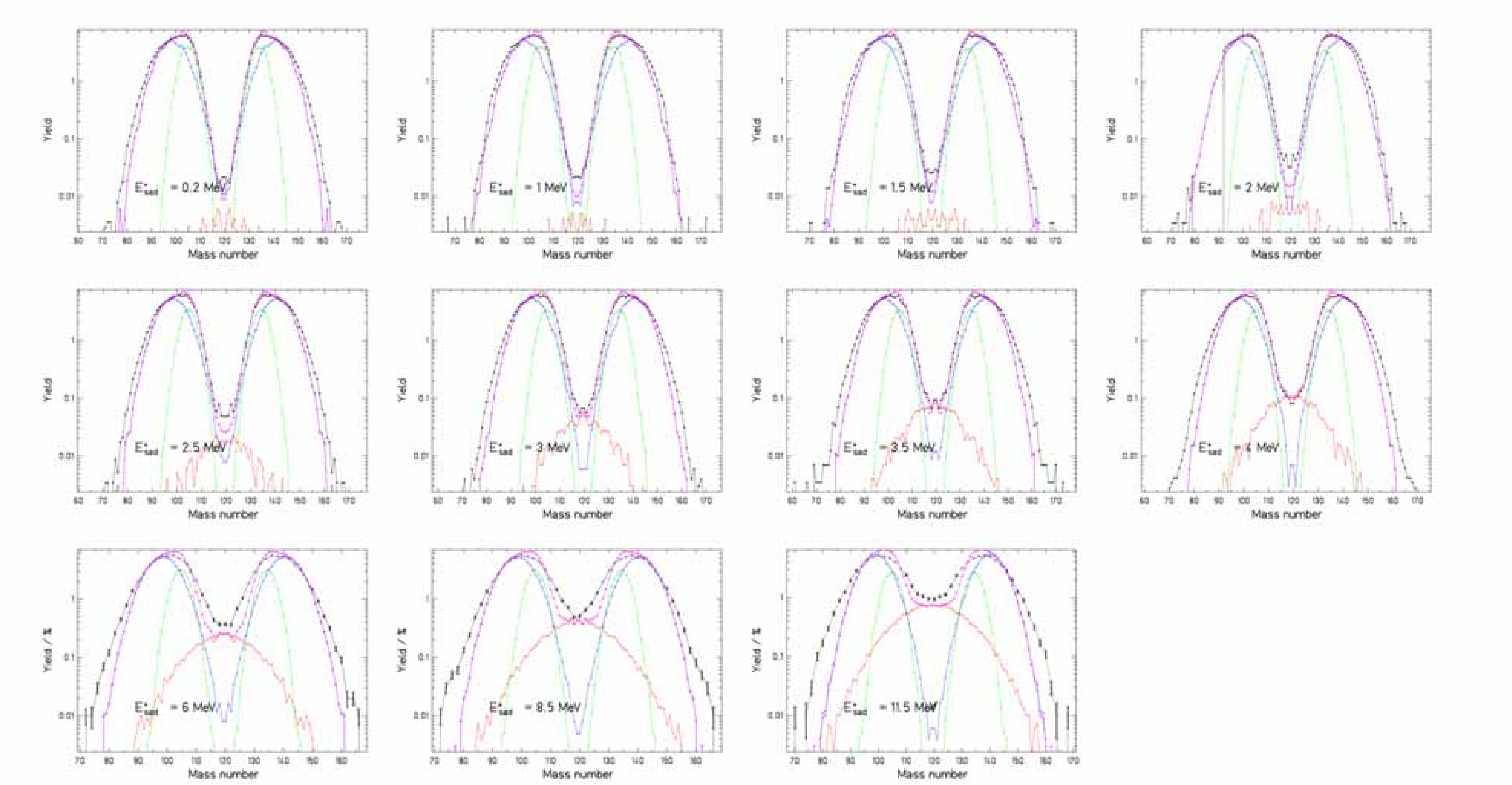

Reproduction ^{238}U (1 *A* GeV) + ^{1}H

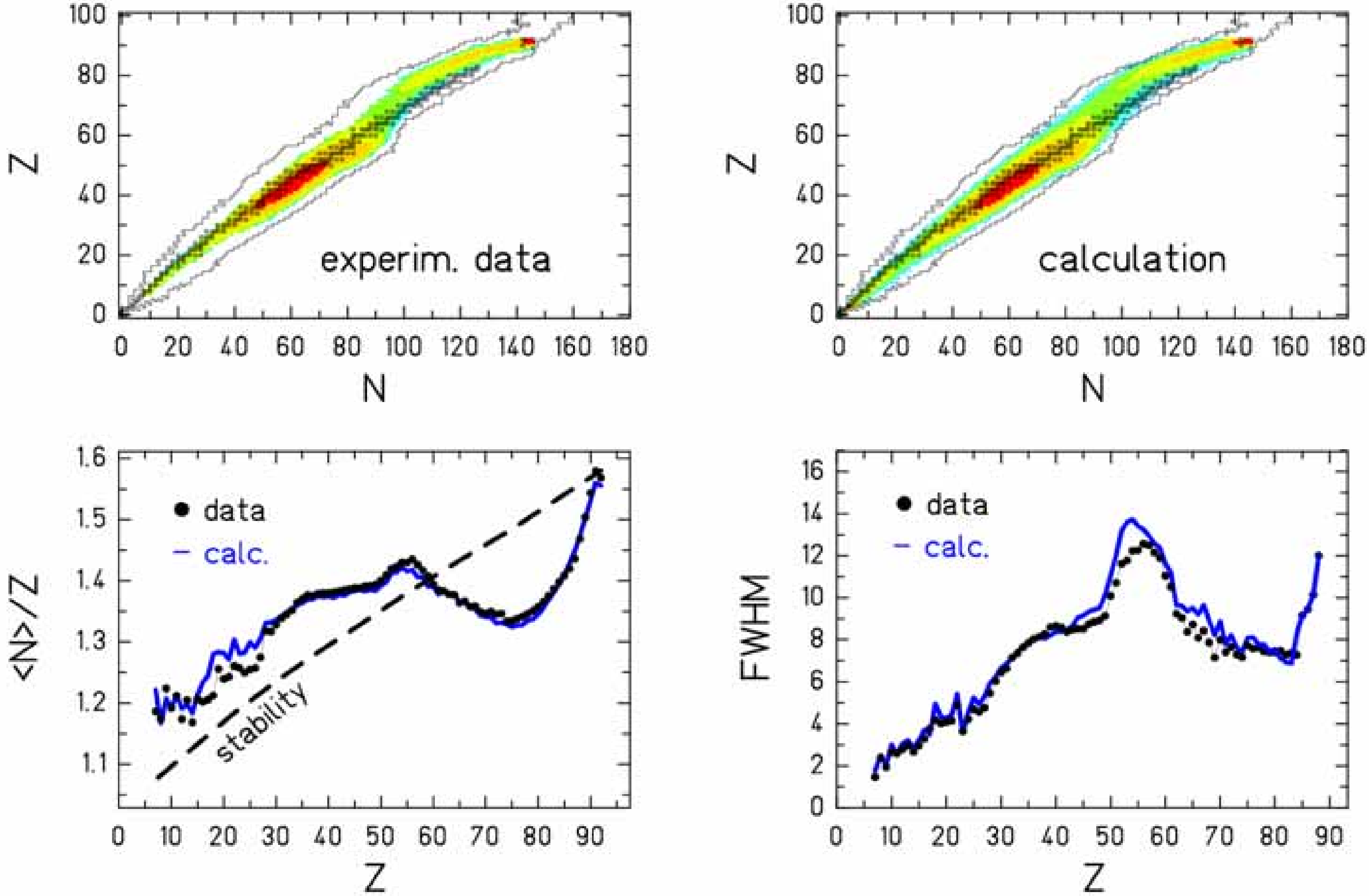

Fission model coupled to spallation – evaporation models

Basic ideas of our macroscopic-microscopic fission approach

(Inspired by Smirenkin, Maruhn, Pashkevich, Rusanov, Itkis, ...)

Macroscopic:

Potential near saddle from exp. mass distributions at high E* (Rusanov)

Macroscopic potential is property of fissioning system (≈ f(Z_{CN}^2/A_{CN}))

Microscopic: assumptions based on 2-centre shell-model calculations (Karpov)

Shells near outer saddle "resemble" shells of final fragments (but weaker)

Properties of shells from exp. nuclide distributions at low E*

Microscopic corrections are properties of fragments (= f(N_f,Z_f))

Dynamics: → approximations based on Langevin calculations (Nadtochy)

τ (mass asymmetry) >> τ (saddle scission) : decision near saddle

τ (N/Z) << τ (saddle scission) : decision near scission

Population of available states with statistical weight (near saddle or scission)

Comparison with other fission models:

Statistical model (A near saddle, N/Z near scission)

(Fong, Wilkins et al. applied the statistical model *at scission*.)

Quantitative population of fission channels

(Brosa proposed a *qualitative* fission-channel approach)

Macroscopic-microscopic approach

(Spirit like Strutinsky approach, but quantitative values *from experiment*)

Macroscopic potential = f(Z_{CN}^2/A_{CN}) / microscopic potential = f(Z_f,N_f)

(Powerful separation and generalisation, *few free parameters, robust extrapol)*)

Disappearance of shell effects

(From systematics of microscopic calculations)

Systematics of model calculations

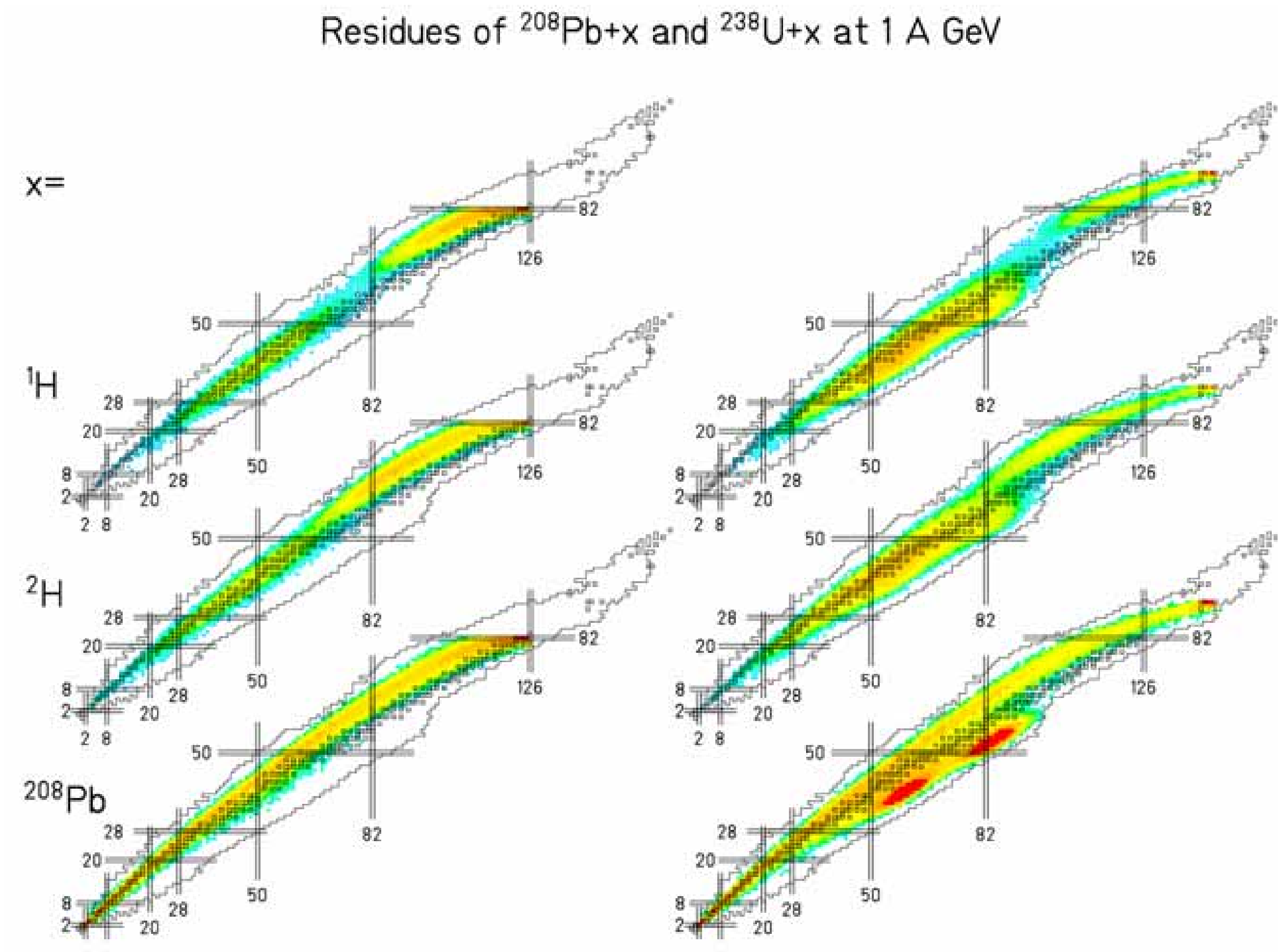

Very different isotopic distributions for different projectile-target combinations!

Experimental data are well reproduced.

Large-acceptance spectrometer (in preparation)

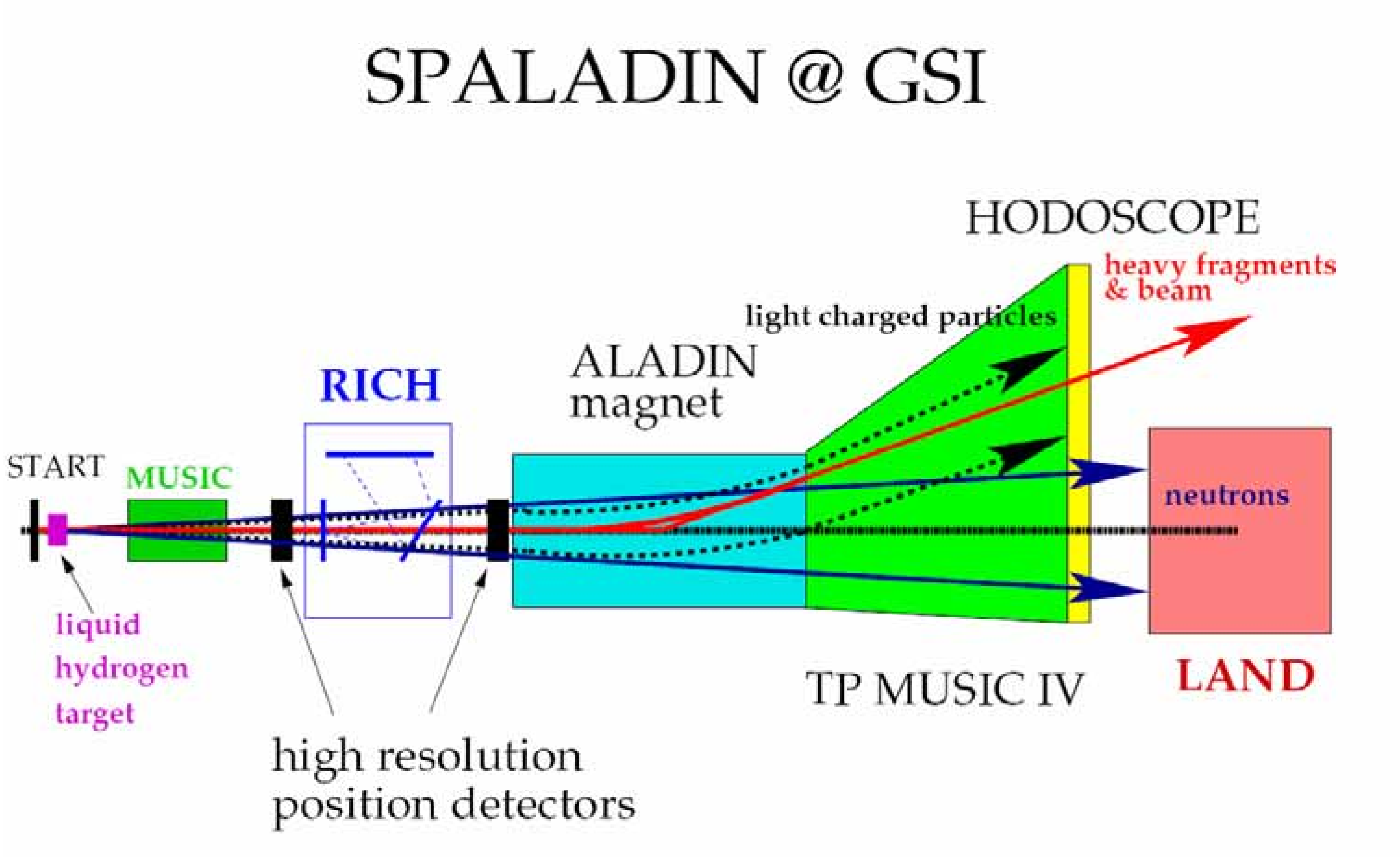

Detection of neutrons, charged particles / but limited mass resolution

The FAIR project

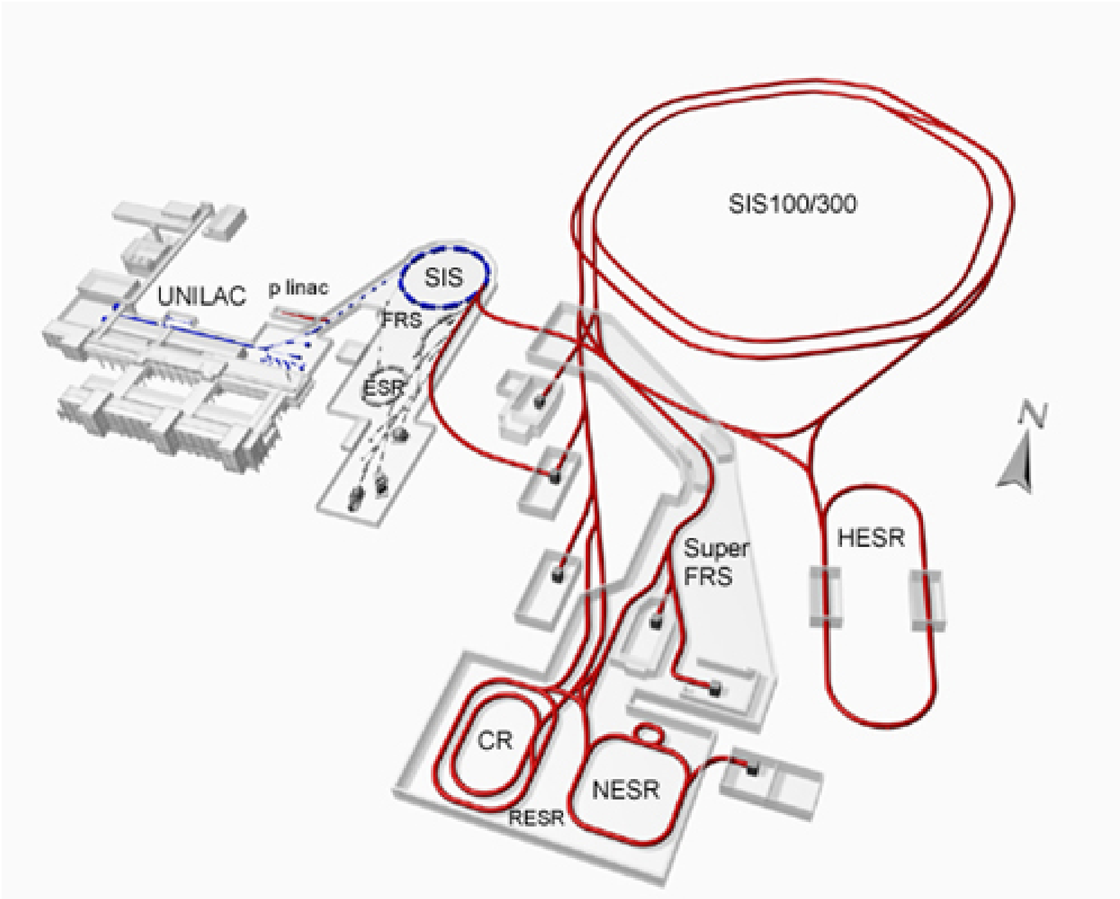

Beams with higher energy and higher intensity

Spectrometers with larger acceptance / higher resolution

Storage rings, electron — ion collider

Electron-ion collider – the ideal tool ?

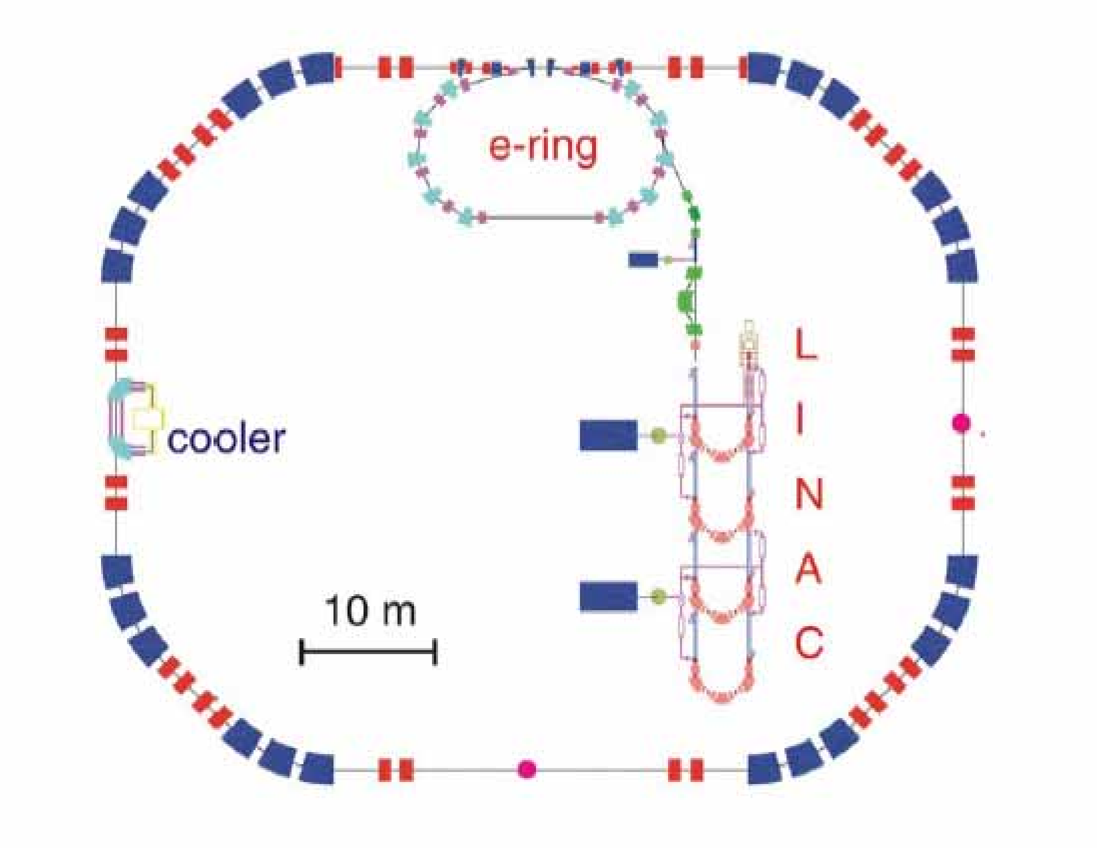

Determination of the excitation energy by inelastic electron electron scattering.

No angular straggling in target.
No contribution from nuclear reactions.

Needs of a spectrometer with large acceptance for the fission fragments.

Conclusion

- The HI-accelerator and spectrometer complex of GSI Darmstadt is unique world-wide
- Experimental progress due to application of inverse kinematics
- Multimodal fission around ^{226}Th studied in detail
- Break-through in measuring full nuclide distributions in spallation reactions in a French-Spanish-German collaboration
- Comprehensive data tables established (→ www-w2k.gsi.de/charms)
- New insight into global features of spallation and fission
- Model for nuclide production in fission on the basis of E_{pot} and ρ
- Successful modelling of all aspects of spallation-fission reactions
- Even better experimental conditions in the future FAIR facility

The CHARMS collaboration

Peter Armbruster, Antoine Bacquias, Lydie Giot, Vladimir Henzl, Daniela Henzlova, Aleksandra Kelić, Strahinja Lukić, Pavel Nadtochy, Radek Pleskač, Maria Valentina Ricciardi, Karl-Heinz Schmidt, Florence Vivès , Bernd Voss, Orlin Yordanov
GSI, Planckstr. 1, D-64291 Darmstadt, Germany

Laurent Audouin, Charles-Olivier Bacri, Monique Bernas, Brahim Mustapha, Claude Stéphan, Laurent Tassan-Got
IPN Orsay, B.P. n. 1, F-91406 Orsay, France

Alain Boudard, Jean-Erique Ducret, Beatriz Fernandez, Sylvie Leray, Claude Volant, Carmen Villagrasa, Wojczek Wlaslo
DAPNIA/SPhN, CEA Saclay, F-91191 Gif sur Yvette Cedex, France

Julien Taieb
DEN/DM2S/SERMA/LENR, CEA Saclay, F-91191 Gif sur Yvette Cedex, France

Christelle Schmitt
IPNL, Université Lyon, Groupe Matiere Nucleaire, 4, rue Enrico Fermi, F-69622 Villeurbanne Cedex, France

Serge Czajkowski, Beatriz Jurado, Michael Pravikoff
CENBG, Le Haut Vigneau, F-33175 Bordeaux-Gradignan, Cedex, France

Paolo Napolitani, Fanny Rejmund
GANIL, B.P. 5027, F-14076 Caen Cedex 5, France

Jose Benlliure, Jorge Pereira, Enrique Casarejos, Manuel Fernandez, Teresa Kurtukian
Univ. Santiago de Compostela, E-15706 Santiago de Compostela, Spain

Arnd Junghans
Forschungszentrum Rossendorf, Postfach 510119, D-01314 Dresden, Germany